Focal length control of complex harmonic and complex pulsed ultrasonic bounded beams

Nico F. Declercq[a] and Joris Degrieck
Soete Laboratory, Department of Mechanical Construction and Production, Ghent University, Sint Pietersnieuwstraat 41, 9000 Gent, Belgium

Oswald Leroy
Interdisciplinary Research Center, Katholieke Universiteit Leuven Campus Kortrijk, Etienne Sabbelaan 53, 8500 Kortrijk, Belgium

(Received 2 September 2004; accepted 2 December 2004; published online 9 February 2005)

This article describes a way to change the focal length of a single transducer without phased array technology and without changing the (real) frequency. The physical effect is induced by changing the signal's amplitude in a precise manner in order to approach the complex harmonic wave regime. In this regime, changing the imaginary frequency results in a change of the focal length. A study is performed for different beam shapes and for complex harmonic signals as well as for complex pulsed signals. © *2005 American Institute of Physics*. [DOI: 10.1063/1.1851015]

I. INTRODUCTION

Focused transducers are widely used in acoustic microscopy[1] and, in general, nondestructive testing.[2–4] In the medical field, pulsed focused ultrasound has long been used to destroy kidney stones, and the high intensity focused ultrasound (HIFU) technique is applied in the treatment of cancer[5] and internal wounds. The latter is realized by "stimulating" thrombocytes to locally coagulate;[6–9] i.e., acoustic hemostasis. The technique is also used to seal air leaks in lungs.[10] It is also possible to treat cancer by means of the local hyperthermia technique, in which low(er) intensity focused ultrasound is used during a much longer period of time. For the moment, one is limited to the use of single focused transducers, which have almost no flexibility to change the focal length, or phased arrays, which are more flexible but possess their own inherent shortcomings, such as a very high cost.

For a given single transducer, the only known technique to change the focal length for a given medium is changing the input frequency. However, unless the new frequency is an odd number of the transducer's first harmonic, the generated power is negligible. The current article describes a technique to change the focal length without changing the frequency, but by altering the amplitude in a very distinctive manner. In what follows, we redefine the word frequency. What is classically called "frequency" is now explicitly called "real frequency." The real frequency is a specific part of a more general "complex frequency" and is responsible for the phase of the considered signal. The "imaginary frequency" is, as will be explained further subsequently, responsible for the temporal amplitude change.

Furthermore, even though focusing of ultrasound is often accompanied by nonlinear effects, especially when very high amplitudes are involved, such as in HIFU, for simplicity, we limit this discourse to a linear regime in viscoelastic media.

[a]Author to whom correspondence should be addressed; electronic mail: [NicoF.Declercq@UGent.be] or [declercq@ieee.org].

II. THEORY

In the linear elasticity regime, sound fields can be divided into the long-lasting or the harmonic type and the short-time, pulsed type. In practice, all sound fields are bounded in space, whereas mathematically, infinite waves are also possible.

A. Building blocks of the bounded beam description

Harmonic infinite plane waves are orthogonal solutions of the wave equation and therefore form the building blocks for the description of complicated sound fields. However, more sophisticated, although more general, solutions of the wave equation are so-called complex harmonic inhomogeneous plane waves. Such waves are described as classical homogeneous plane waves, as

$$\varphi(r,t) = A\mathbf{P}\exp(\gamma\mathbf{k}\cdot\mathbf{r} - 2\pi\gamma f t) \text{ with } \gamma = \pm 1, \tag{1}$$

except that each of the quantities in Eq. (1), apart from time t and position $\mathbf{r}$, are complex valued instead of simply real valued. An extensive historical overview of such waves has recently been reported by Declercq *et al.*[11]

Besides the amplitude A, the polarization is, in general, complex valued, as

$$\mathbf{P} = \mathbf{P}_1 + i\mathbf{P}_2, \tag{2}$$

and so is the frequency f, as

$$f = 2\pi(f_{\mathrm{Re}} + if_{\mathrm{Im}}). \tag{3}$$

The complex wave vector is decomposed as[11]

$$\mathbf{k} = \mathbf{k}_{\mathrm{Re}} + i\mathbf{k}_{\mathrm{Im}} = \mathbf{k}_{\mathrm{Re}} + i(\boldsymbol{\alpha} - \boldsymbol{\beta}), \tag{4}$$

with $\boldsymbol{\alpha} \| \mathbf{k}_{\mathrm{Re}}$ and $\boldsymbol{\beta} \perp \mathbf{k}_{\mathrm{Re}}$. It can then be verified that

$$\mathbf{u} = A\mathbf{P}\exp(2\pi\gamma f_{\mathrm{Im}}t)\exp(-\gamma\boldsymbol{\alpha}\cdot\mathbf{r}) \times\exp(\gamma\boldsymbol{\beta}\cdot\mathbf{r})\exp i(\gamma\mathbf{k}_{\mathrm{Re}}\cdot\mathbf{r} - 2\pi\gamma f_{\mathrm{Re}}t). \tag{5}$$

The parameter $\mathbf{k}_{\mathrm{Re}}$ is the propagation wave vector, f_{Re} is the real frequency, $\boldsymbol{\alpha}$ is the damping vector, and $\boldsymbol{\beta}$ is the inho-

mogeneity vector. The parameter γ is included in Eqs. (1) and (5) and determines the sign convention that is used. Most often it is set equal to +1, although some researchers prefer to set it equal to −1. The need to distinguish between different values of γ will be clear later on, when we describe focusing of bounded beams. The parameter f_{Im} determines the transient feature of the wave under consideration and is called the source parameter. If γf_{Im} is positive, the wave is amplified in time; if it is negative, the wave diminishes in time.

If we take a closer look at Eq. (5), we see that only the last factor determines the phase of the complex harmonic inhomogeneous wave. All the other factors determine the amplitude. Nevertheless, Eq. (5) must be a solution of the wave equation, because otherwise it cannot physically exist.

For viscoelastic media, the wave equation for waves described by Eq. (1) results in the dispersion relation;[11] i.e.,

$$\mathbf{k}\cdot\mathbf{k}=\left(\frac{2\pi f}{v_b}-i\alpha_{0,b}\right)^2, \tag{6}$$

where $b=d$ for longitudinal waves and $b=s$ for shear waves. v_b is the phase velocity for harmonic homogeneous plane waves (i.e., having a real wave vector and real frequency) and $\alpha_{0,b}$ is the intrinsic damping coefficient. Contrary to a harmonic wave, whose amplitude is constant in time and contains only one single (real) frequency f_{Re}, a complex harmonic wave shows exponential amplitude decay in time and contains one single complex frequency $f=f_{\mathrm{Re}}+if_{\mathrm{Im}}$. The generation of complex harmonic waves has already been achieved experimentally[12] by application of a proper electrical input signal to a single transducer.

Recently, it has been shown[11,13] that, for complex harmonic waves, it is necessary to distinguish between phase velocity

$$v_{\mathrm{ph}}=\frac{2\pi f_{\mathrm{Re}}}{\mathbf{k}_{\mathrm{Re}}\cdot\mathbf{k}_{\mathrm{Re}}}\mathbf{k}_{\mathrm{Re}} \tag{7}$$

and amplitude velocity

$$v_{\mathrm{amp}}=\frac{2\pi f_{\mathrm{Im}}}{\mathbf{k}_{\mathrm{Im}}\cdot\mathbf{k}_{\mathrm{Im}}}\mathbf{k}_{\mathrm{Im}}. \tag{8}$$

The velocity of energy propagation is then given by

$$\mathbf{v}_E=\frac{\mathbf{S}_{\mathrm{Re}}}{\mathbf{S}_{\mathrm{Re}}\cdot\mathbf{S}_{\mathrm{ph}}}, \tag{9}$$

with phase slowness vector $\mathbf{S}_{\mathrm{ph}}$ given by[11]

$$\mathbf{S}_{\mathrm{ph}}=\frac{\mathbf{k}_{\mathrm{Re}}}{2\pi f_{\mathrm{Re}}}, \tag{10}$$

and with $\mathbf{S}_{\mathrm{Re}}$ the real part of the slowness vector, defined as[11]

$$\mathbf{S}_{\mathrm{Re}}=(\mathbf{k}_{\mathrm{Im}}f_{\mathrm{Im}}+\mathbf{k}_{\mathrm{Re}}f_{\mathrm{Re}})/2\pi(f_{\mathrm{Re}}^2+f_{\mathrm{Im}}^2). \tag{11}$$

B. Bounded beam description

A bounded sound beam is determined by a profile along the direction perpendicular to the sound propagation direction, and a propagation pattern determined by physical laws.

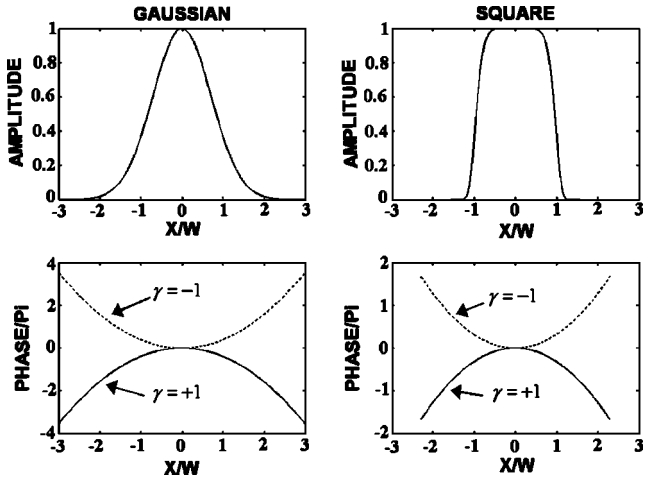

FIG. 1. Graphical representation of a Gaussian and a square profile, in amplitude as well as in phase.

In isotropic homogeneous media, the properties of a real three-dimensional (3D) bounded beam are sufficiently represented by a two-dimensional (2D) bounded beam. This approach has been followed in many papers before.[14–33] Therefore, we assume a bounded beam having a given profile along the x direction and propagating in the z direction. Furthermore, this assumption involves constant properties along the y direction and results in relative numerical and representational ease.

The profile (along the x direction) of a focused bounded harmonic beam $g(x,z,t,f_{\mathrm{Re}},f_{\mathrm{Im}})$, i.e., Gaussian[34] if $\xi=2$, or square if $\xi=8$, can be described as

$$g(x,0,0,f_{\mathrm{Re}},f_{\mathrm{Im}})=\exp(-x^{\xi}/W^{\xi})\exp[-\gamma ix^2/(W^2W_{\mathrm{foc}}^2)], \tag{12}$$

W being the (Gaussian) beam width and W_{foc} being a focusing parameter. For unfocused beams, $W_{\mathrm{foc}}=\infty$, whereas for focused beams, W_{foc} is typically smaller than or equal to unity. The profile (12) shows amplitude as well as phase variation. The result can be seen in Fig. 1, for a Gaussian beam profile ($\xi=2$, $W=4$ mm, $W_{\mathrm{foc}}=0.9$) and a square profile ($\xi=8$, $W=4$ mm, $W_{\mathrm{foc}}=1$). Here, it is necessary to distinguish between the positive sign choice ($\gamma=\pm1$)) and the negative sign choice ($\gamma=-1$) in the building blocks (1) and (5) and the profile (12). The reason is that focusing occurs when the center of the beam is behind in time, compared to the edges of the beam. This principle is incorporated by a positive or a negative phase shift of the center compared to the edges, depending on whether the material particle vibrations are represented by a clockwise (or counterclockwise, respectively) rotating phase vector in the complex phase space.

For the moment, we deal with (complex) harmonic beams, which means that there is only one (complex) frequency involved. Later on, when pulsed beams are considered, more frequencies will be involved through a temporal Fourier transform.

Because a Gaussian function is not a solution of the wave equation, it is necessary to decompose the profile function (12) into plane waves, i.e.,

$$g(x,z,t,f_{\mathrm{Re}},f_{\mathrm{Im}}) = \left[\sum_{m=-M}^{M} A_m \exp i\gamma(k_x^m x + k_z^m z)\right] \times \exp[-2\pi\gamma(f_{\mathrm{Re}} + if_{\mathrm{Im}})t], \quad \text{with } k_x^m = mk_x^1 \in \mathbb{R}, \tag{13}$$

using the spatial discrete Fourier transform for obtaining the Fourier coefficients A_m and the wave vector components k_x^m and applying the dispersion relation (6) in order to obtain the remaining wave vector components k_z^m. The value of k_x^1 depends on the considered spatial interval and will be explained later.

Given the values k_x^m, obtained from the discrete Fourier transform, each wave vector component k_z^m determines the propagation direction of the plane wave denoted by the integer m and is a function of the complex frequency f through the dispersion relation (6). The effect of the phase profile of the bounded beam (see bottom of Fig. 1) on the propagation structure, also depends on the frequency. This effect is well known for the concept of real frequencies. If a focused transducer is driven at different real frequencies, the focal length changes because the propagation direction of the present Fourier components change as well. However, driving a given transducer is often only possible at frequencies near a given first harmonic or at odd multiples. Nevertheless, the effect of a change of the complex frequency, and in particular of the source parameter f_{Im}, on the focal length, is unknown. Because changing f_{Im} actually does not mean applying a different driving frequency, but essentially means relaxation of the input signal. The influence on the focal length of the input signal relaxation is of practical interest. The next section describes the effect of the source parameter f_{Im} on the focal length of a complex harmonic Gaussian beam and also of a square beam.

III. COMPLEX HARMONIC FOCUSED BOUNDED BEAMS

From a mathematical point of view, harmonic bounded beams are easily described, because they can be decomposed into Fourier components having the same (complex) frequency [Eq. (13)]. The situation of pulsed bounded beams will be dealt with in the next paragraph. We take the example of focused bounded beams in water. The longitudinal wave velocity v is 1480 m/s. For simplicity, except when explicitly stated, we reckon only with a lossless liquid; i.e., $\alpha_{0,d}=0$. The real frequency is 2 MHz. We define the focal length as the distance between the origin and the spot of highest amplitude within the focused beam. Because the profile of a bounded beam is, by definition, described by a function that differs from zero within a limited spatial interval, the fast Fourier transform (FFT) method is applicable. The spatial interval of the transform must be chosen large enough because the resulting representation is automatically periodic in space, with a period equal to that spatial interval, and we want to avoid interference, along the propagation path, between neighboring beams in the mathematical representation. For that reason, we have chosen a large spatial interval $[-20W, 20W]$. This spatial interval determines the lower bound of the considered nonzero values of $|k_x^m|$; i.e., $k_x^1 = 2\pi/40W$. The upper bound is determined by Nyquist–Shannon's theorem.[35–37] Very briefly, Nyquist–Shannon's theorem states that, when sampling at a given rate, the highest frequency that can appear in the sampled signal is half the sampling frequency. In the considered interval $[-20W, 20W]$, we found for our purposes, that the beam profile could sufficiently well be represented by 2^{12} points, involving, when translating Nyquist–Shannon's theorem to spatial samples, an upper bound for k_x^m of $2\pi/40W \times 2^{11}$. We choose powers of 2, because the FFT is much faster for a number of samples being equal to a power of 2.

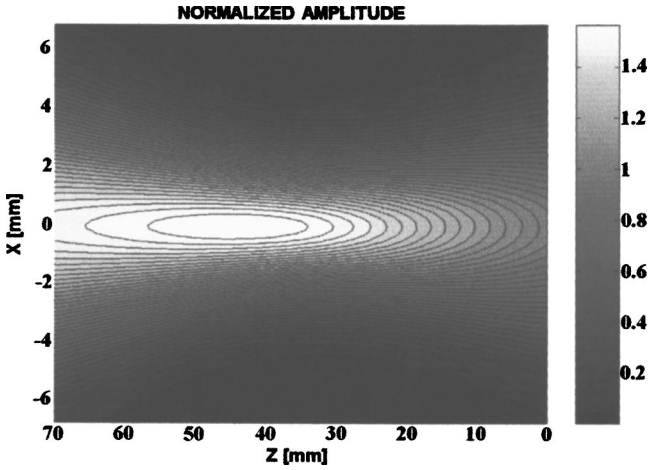

FIG. 2. Filled contour plot of the amplitude pattern of a complex harmonic bounded Gaussian beam in water, originating at $(x,z)=(0,0)$, and characterized by $W=4$ mm, $W_f=0.9$, $f_{\mathrm{Re}}=2$ MHz, and $f_{\mathrm{Im}}=-1500$ Hz. The focal spot is situated at $z\approx 48$ mm. In this figure, sound is propagating from right to left.

A. Focused Gaussian beams

First of all, a filled contour plot displays isolines calculated from the amplitude distribution and fills the areas between the isolines using constant colors. In Fig. 2, a filled contour plot of the amplitude pattern of the Gaussian bounded beam in water, originating at $(x,z)=(0,0)$, is shown, characterized by $W=4$ mm, $W_f=0.9$, $f_{\mathrm{Re}}=2$ MHz, and $f_{\mathrm{Im}}=-1500$ Hz. It is seen that the focal spot is situated at $z\approx 48$ mm. The pattern for the case of $f_{\mathrm{Im}}=1500$ Hz is shown in Fig. 3, where it is seen that the focal spot is situated at $z\approx 20$ mm. The difference in focal spot position is significant. In fact, in Fig. 4, the focal spot position is calculated as a function of f_{Im}, and it is seen that the focal length changes when altering f_{Im}. The change is remarkable and spans over 4 cm. This is as good as what is to be expected from a phased array transducer of comparable size that is used in HIFU.[38] We have repeated the calculations for a nonzero damping $\alpha_{0,d}=p\alpha_w$, with $\alpha_w=0.6\times 10^{-15}$, the damping in physical water, and with $p\in\{0,5,\ldots,50\}$. Even though damping influences the amplitude at the focal spot, no change was noticeable in the focal length. For this Gaussian beam, we have also calculated the focal length as a function of f_{Re} for $f_{\mathrm{Im}}=0$, and we have found that beyond a threshold

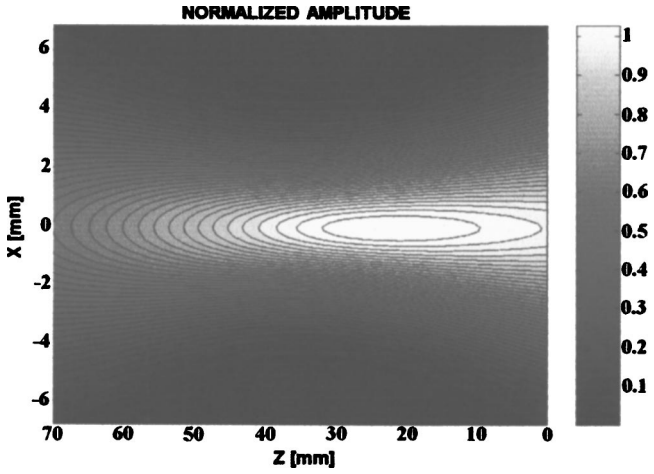

FIG. 3. Similar to Fig. 2, except that $f_{\mathrm{Im}}=1500$ Hz. Here, the focal spot is situated at $z\approx 20$ mm. In this figure, sound is propagating from right to left.

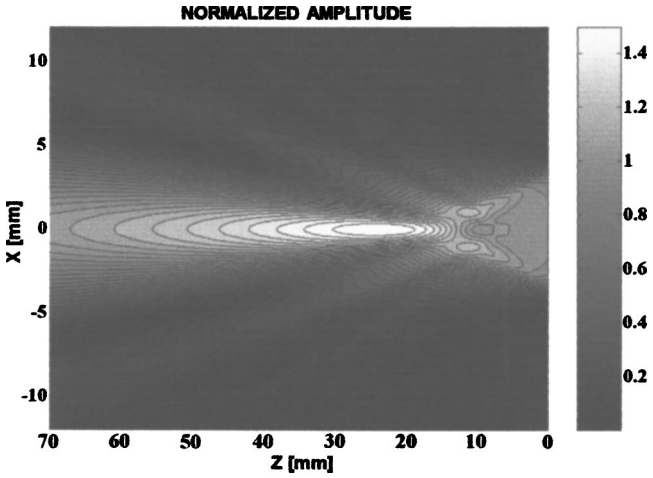

FIG. 5. Amplitude propagation pattern of a complex harmonic bounded square-shaped beam in water originating at (0,0), characterized by $W=4$ mm, $W_f=1$, $f_{\mathrm{Re}}=2$ MHz, and $f_{\mathrm{Im}}=-100$ Hz. The focal spot is situated at 23.4 mm. In this figure, sound is propagating from right to left.

frequency of 0.5 MHz, the distance D (in mm) of the focal spot is given by a linear function of f_{Re} (in MHz) described by

$$D = 16.77 f_{\mathrm{Re}} - 0.8534. \tag{14}$$

The existence of a threshold frequency is due to a considerable near field for low frequencies. As stated earlier, changing f_{Re} is in practice not always realistic, even though mathematically, a considerable focal shift is possible, as seen in Eq. (14).

B. Focused square beams

In order to show that the effect of the focal length change is not just a mathematical trick that is only valid for Gaussian beams, we have performed similar calculations as in the previous section, for a square profiled bounded beam, as depicted on the right side of Fig. 1.

In Fig. 5, the amplitude pattern of the square shaped bounded beam in water originating at (0,0) is shown, characterized by $W=4$ mm, $W_f=1$, $f_{\mathrm{Re}}=2$ MHz, and $f_{\mathrm{Im}}=-100$ Hz. The focal spot is situated at 23.4 mm. In Fig. 6, the change of focal length as a function of f_{Im} is given. Even though the change in focal spot distance as a function of f_{Im} and the interval in which focalization occurs, is different from the case of a Gaussian beam (cf. Fig. 4), the effect of f_{Im} is again significant. It is therefore shown that f_{Im} does not solely influence the focal length of Gaussian beams, but also of other types.

IV. COMPLEX PULSED FOCUSED BOUNDED BEAMS

A. Signal representation

The previous paragraph described focusing of complex harmonic beams. Such beams are mathematically very elegant, although they never exist in reality. Real signals are always limited in time and they can only be approximated by a (complex) harmonic beam within a restricted time interval that is smaller than the duration of the signal. A very short signal is generally called a pulse and is classically generated by means of a capacitor unloading its charge rapidly to a transducer. By complex pulsed signals, we actually mean a somewhat longer signal that approaches the complex harmonic signal structure within a limited temporal interval. Therefore, there is a complex harmonic regime, preceded by a start regime and followed by a stop regime. The start re-

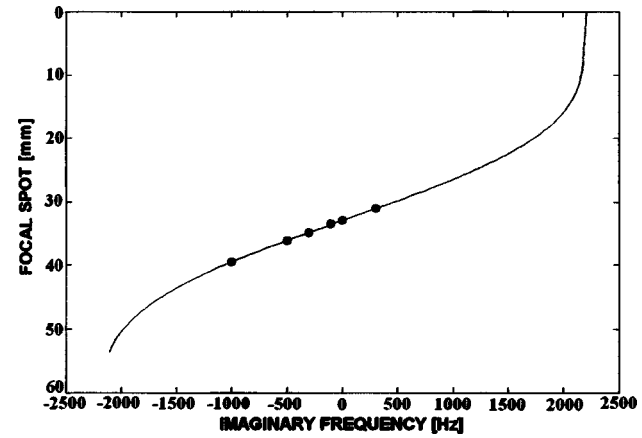

FIG. 4. Focal length of a complex harmonic Gaussian beam in water as a function of f_{Im} and for $W=4$ mm, $W_f=0.9$, and $f_{\mathrm{Re}}=2$ MHz.

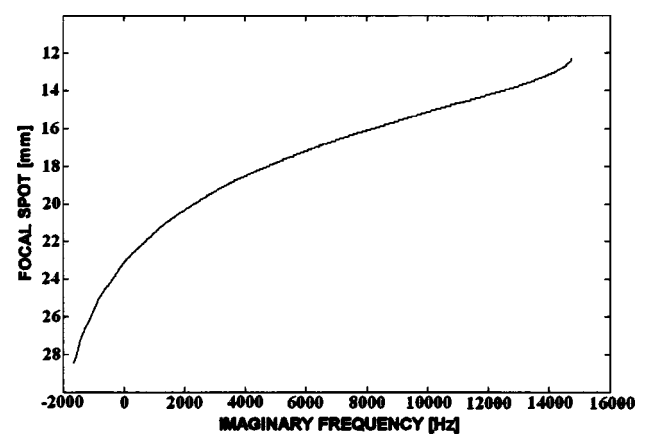

FIG. 6. Focal length of a complex harmonic square-shaped beam in water as a function of f_{Im} and for $W=4$ mm, $W_f=1$, and $f_{\mathrm{Re}}=2$ MHz.

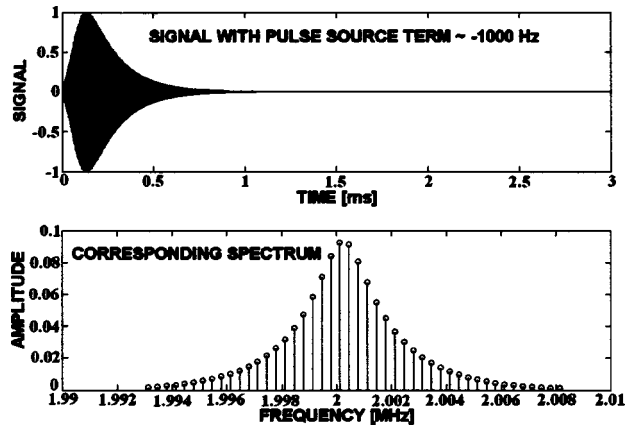

FIG. 7. Top: complex pulsed signal given by Eq. (15), for $f=2$ MHz $-i1000$ Hz and a duration of 2 ms. Bottom: The corresponding Fourier spectrum.

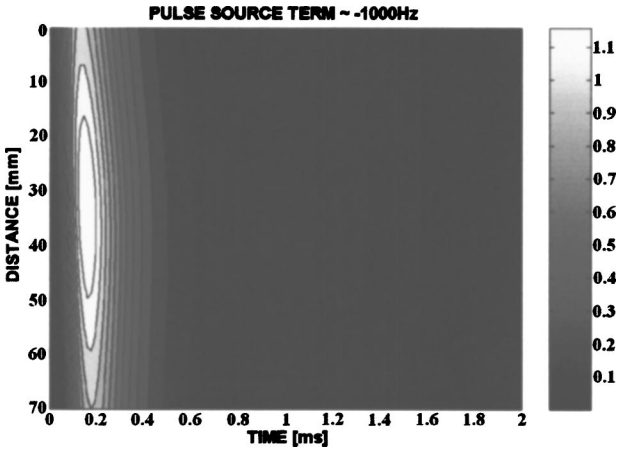

FIG. 8. Amplitude profile along the Z axis ($x=0$) for 125 instants of time from the beginning to the end of the signal of Fig. 7. In the complex harmonic regime, the presence of a focal spot is clear and the focal length corresponds to that of the corresponding complex harmonic bounded beam.

gime is characterized by a relatively rapid increase of the amplitude from zero to a start maximum, whereas the stop regime has the opposite effect. A realistic function that describes complex pulsed signals is given by

$$h(t) = \exp\left[-\left(\frac{t-1.08m}{m}\right)^{18}\right] \times \exp\left[-i\gamma 2\pi f\left(t-\frac{1}{4f_{\mathrm{Re}}}\right)\right], \tag{15}$$

where $m=0.455/R$, with R the pulse rate and $1/R$ the duration of the complex harmonic pulse. The symbol γ is defined earlier and represents the sign choice of the wave description. Because the signal (15) is not a solution of the wave equation, a decomposition into Fourier components is again mandatory. In this perspective, it is necessary to paraphrase Nyquist–Shannon's theorem[35–37] as "the sampling rate must be equal to, or greater than, twice the highest frequency component in the signal." We considered a pulse rate of $(2\ \mathrm{ms})^{-1}$, which means that the considered pulses cannot last longer than 2 ms. We have again used $f_{\mathrm{Re}}=2$ MHz and several numerical simulations revealed that the frequency components of the considered time limited signals are always situated in the short vicinity of the central frequency of 2 MHz. We therefore limit the upper frequency to $(2+\delta)$ MHz. Nyquist–Shannon's theorem shows that the sampling rate must then be larger than $(4+2\delta)$ MHz, or, given the pulse rate of $(2\ \mathrm{ms})^{-1}$, the number of samples must be $8000+4000\delta$. Several trial calculations showed that the frequency components, for the signals tackled in this article, are always negligible above a value determined by $\delta=0.048$. This value results in a number of samples given by $2N=2^{13}$. Therefore, N is the number of Fourier components and the time-limited signal $h(t)$ is represented by

$$h(t) = \sum_{n=0}^{N} B_n \exp(-i2\pi f_n t), \quad \text{with } f_n = nR \in \mathbb{R}. \tag{16}$$

A first example of a complex pulsed signal is given in Fig. 7, for $f=2$ MHz $-i1000$ Hz and a duration of 2 ms. The corresponding Fourier spectrum is also given in Fig. 7. It can be seen that the relevant frequency components are distributed in a very small range around the central frequency of 2 MHz. We would like to point out that a signal that is described by a complex frequency, can always be represented by a summation of signals having a real frequency, if it is a time-limited signal. Furthermore, the distribution of the frequency components around the real part of the considered complex frequency, depends on the imaginary part. The effect of changes in the focal length is then understood as follows: The presence of different frequency components in the Fourier spectrum causes a different propagation pattern, as described earlier. In Fig. 7, the amplitude of the considered complex pulse, shows a maximum at a certain position in time. The side left of the maximum is called the "start regime," whereas the side right of the maximum is the "complex harmonic regime." The stop regime is situated near 2 ms, and is invisible here, because the amplitude of the signal has dropped so much in the complex harmonic regime.

B. Bounded beam representation

The description of a bounded beam that is generated by an input complex pulsed signal at the origin, is performed by a superposition of harmonic plane waves as follows:

$$g(x,z,t,f_{\mathrm{Re}},f_{\mathrm{Im}}) = \sum_{m=-M}^{M}\sum_{n=0}^{N} C_{m,n}\exp i(k_x^m x + k_z^{m,n} z - 2\pi f_n t), k_x^m, f_n \in \mathbb{R}. \tag{17}$$

If $C_{m,n}$ is rewritten as

$$C_{m,n} = a_m b_n, \tag{18}$$

then, identification with the expression within the brackets of Eq. (13) and with Eq. (16) results in $a_m=A_m$, $b_m=B_m$, and $k_z^{m,n}$ is determined by k_x^m and f_n through the dispersion equation (6). Actually, this means that the number of plane waves in the decomposition equation (17) is the product of the number in Eq. (13) for the spatial description and in Eq. (16) for the temporal description, which means that we are dealing with 2^{24} samples, or in other words, more than 8×10^6

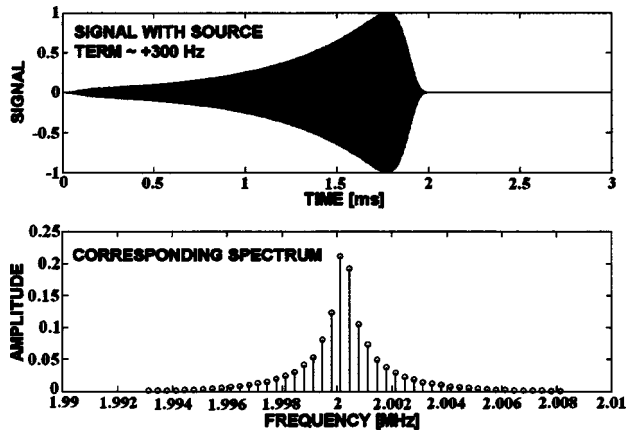

FIG. 9. Same as Fig. 7, except that the the frequency is now $f=2$ MHz $+i300$ Hz. This corresponds to a complex pulse having increasing amplitude.

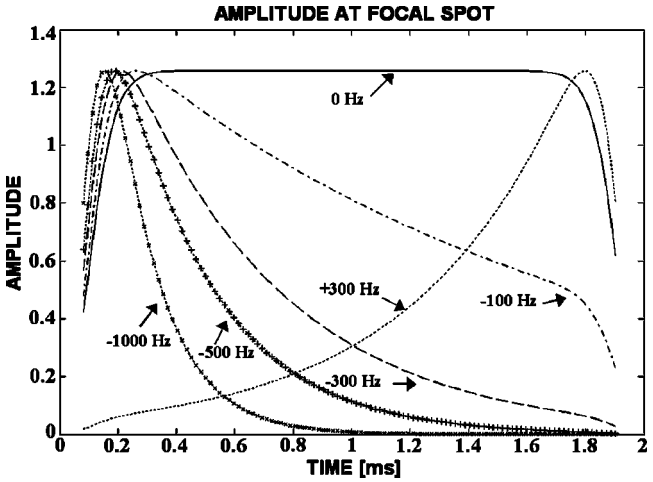

FIG. 11. The amplitude at the focal spot for each instant of time and for six cases that correspond to the bold dots of Fig. 4.

building blocks that, when superposed, form the considered bounded, pulsed beams. This results in a relatively large computation time. It is clear that a similar description of 3D beams would require far too much calculation time, which is an additional reason only 2D bounded beams are considered here.

Numerical implementation of Eq. (17) enables us to visualize the beam pattern at any instant in time. Because this article primarily highlights focusing of bounded beams, we show, by means of a filled contour plot in Fig. 8, the amplitude profile along the Z axis ($x=0$) for 125 instants of time from the beginning to the end of the signal of Fig. 7. It can be seen that, as soon as the complex harmonic regime is reached, a stable focusing effect occurs at a distance equal to the one for complex harmonic bounded beams characterized by the same beam width, focusing parameter and complex frequency. In fact, the focal length in the complex harmonic regime was calculated for different values of the imaginary frequency. The results are added to Fig. 4 as bold dots. The signal, corresponding to an imaginary frequency of 300 Hz, is given in Fig. 9. Its spatial structure along the z axis for each instant of time is given in Fig. 10. Again, in the complex harmonic regime, a focal spot is visible at the position corresponding to the case of a complex harmonic beam. The focus disappears in the stop regime. The stop regime is significant here, because, contrary to the signal in Figs. 7 and 8, this signal increases its amplitude before reaching the stop regime.

It is also clear that the amplitude at the focal spot, changes in time due to the shape of the complex pulse. In Fig. 11, the amplitude at the focal spot is given for each instant of time and for six cases that correspond to the bold dots of Fig. 4. Furthermore, the position of the focal spot is also a function of time, especially in the start and stop regimes. This is seen in Fig. 12, where the line code is the same as in Fig. 11. It is seen that the focal spot position is constant in the complex harmonic regime, and changes in the other regimes and also that the amplitude at the focal spot follows the amplitude of the input signal. An important question to be asked is where such a temporal and spatially limited beam produces the largest power. Of course, it must be on the focal spot, but because the position of the focal spot and the accompanied amplitude both change in time, it is not evident to give an immediate answer. For that reason, we have calculated the following function:

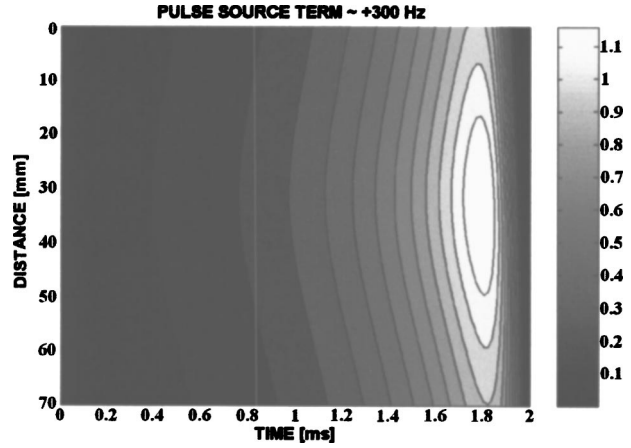

FIG. 10. Same as Fig. 8, except that the frequency is now $f=2$ MHz $+i300$ Hz. This corresponds to a complex pulse having increasing amplitude.

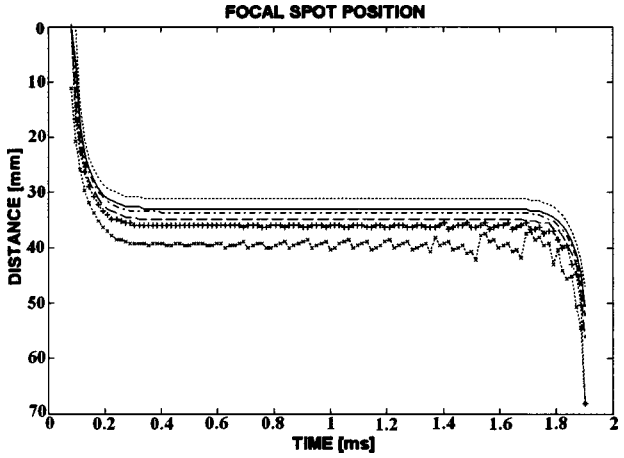

FIG. 12. The position of the focal spot as a function of time, the line code is the same as in Fig. 11.

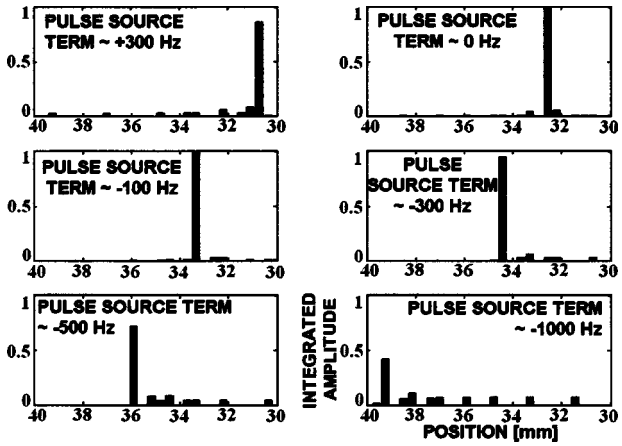

FIG. 13. A measure of the total deliverd power at the focal spot within one complex pulse, as a function of the distance along the *Z* axis, calculated by means of Eq. (19). It is clear that the maximum power release happens at the focal length corresponding to the complex harmonic regime.

$$Q(z,f_{\mathrm{Re}},f_{\mathrm{Im}}) = \int_0^{1/R} \frac{A(z,t,f_{\mathrm{Re}},f_{\mathrm{Im}})}{P(f_{\mathrm{Re}},f_{\mathrm{Im}})} \frac{P(f_{\mathrm{Re}},0)}{\mathrm{H}(f_{\mathrm{Re}})} dt, \tag{19}$$

with

$$P(f_{\mathrm{Re}},f_{\mathrm{Im}}) = \int_0^{1/R} |g(0,0,t,f_{\mathrm{Re}},f_{\mathrm{Im}})| dt \tag{20}$$

being the amplitude of the input signal, integrated over the duration of the complex pulse and characterized by a frequency $f=f_{\mathrm{Re}}+if_{\mathrm{Im}}$. Furthermore,

$$H(f_{\mathrm{Re}}) = \max\left[\int_0^{1/R} A(z,t,f_{\mathrm{Re}},0)dt\right] \tag{21}$$

and

$$A(z,t,f_{\mathrm{Re}},f_{\mathrm{Im}}) = |g(0,z,t,f_{\mathrm{Re}},f_{\mathrm{Im}})|_{\mathrm{FocalSpot}}. \tag{22}$$

The function of Eq. (19) is a measure of the total energy received during the duration of the pulse on a certain spot along the *z* axis, and normalized so that the total power of the input signals under consideration are the same for each of those signals. Figure 13 shows the result for 190 discrete positions along the *z* axis and for incorporation of 125 instants of time. Only the results between 30 and 40 mm are given, because the values were negligible elsewhere. It is seen that, even though the focal spot changes its position in time, and even though the amplitude at the focal spot changes in time, overall, the largest amount of energy is delivered on the constant focal spot in the complex harmonic regime. This is really important, especially when not the peak value of the amplitude at the focal spot is important, but the overall energy delivery, such as in the use of the local hyperthermia technique mentioned in Sec. I.

V. CONCLUSIONS

We have described the influence of the frequency on the focal length of a bounded beam. The effect of the real frequency is well known and has only been given short consideration. More attention was drawn to the effect of the imaginary part of the frequency. This imaginary part is responsible for an exponential change of the amplitude in time and different imaginary frequencies result in different focal lengths. We have shown that this effect happens for Gaussian beams as well as for square beams. We have also shown that the value of the focal length does not depend on the intrinsic damping parameter.

Because real signals are always limited in time, we have also studied complex pulses and have shown that the effect of the imaginary part on the focal length of complex pulsed bounded beams is essentially the same as for complex harmonic bounded beams, except in the start and stop regimes. Even though we only considered a linear regime in an isotropic and homogeneous medium like water, it is likely that similar effects will occur in more complicated media such as human tissue,[39] and that for many applications, especially in the medical field, the cost of equipment may be reduced if for some treatments, expensive phased arrays can be replaced by much cheaper single transducers.

ACKNOWLEDGMENT

The authors are indebted to "The Flemish Institute for the Encouragement of the Scientific and Technological Research in Industry (I.W.T.)" for financial support.

[1] Q. L. Zhang, V. M. Levin, J. Zhang, H. Z. Zhang, J. S. He, S. G. Zhang, and S. P. Liu, Prog. Nat. Sci. **11**, S160 (2001).
[2] D. Fei, D. E. Chimenti, and S. V. Teles, J. Acoust. Soc. Am. **113**, 2599 (2003).
[3] D. E. Chimenti and D. Fei, Int. J. Solids Struct. **39**, 5495 (2002).
[4] K. Yamanaka, J. Appl. Phys. **54**, 4323 (1983).
[5] A. H. Chan, G. Huynh, M. Paun, V. Y. Fujimoto, D. E. Moore, and S. Vaezy, in *Therapeutic Ultrasound, Proceedings of the 2nd International Symposium*, edited by M. A. Andrew, L. A. Crum, and S. Vaezy (American Institute of Physics, Molville, NY, 2003), pp. 391–399.
[6] G. W. Keilman and P. J. Kaczkowski, J. Acoust. Soc. Am. **103**, 2831 (1998).
[7] S. L. Poliachik, P. D. Mourad, L. A. Crum, and W. L. Chandler, J. Acoust. Soc. Am. **107**, 2787 (2000).
[8] L. A. Crum *et al.*, J. Acoust. Soc. Am. **106**, 2228 (1999).
[9] J. H. Hwang, S. Vaezy, R. Martin, M.-Y. Cho, M. L. Noble, L. A. Crum, and M. Kimmey, Gastrointest Endosc **58**, 111 (2003).
[10] S. Vaezy, C. Cornejo, R. Martin, and L. Crum, in *Therapeutic Ultrasound, Proceedings of the 2nd International Symposium*, edited by M. A. Andrew, L. A. Crum, and S. Vaezy (American Institute of Physics, Molville, NY, 2003), pp. 163–167.
[11] N. F. Declercq, R. Briers, J. Degrieck, and O. Leroy (unpublished).
[12] M. Deschamps and O. Poncelet, J. Acoust. Soc. Am. **107**, 3120 (2000).
[13] O. Poncelet and M. Deschamps, J. Acoust. Soc. Am. **102**, 292 (1997);, O. Poncelet, PhD thesis, University of Bordeaux 1, 1996.
[14] J. M. Claeys and O. Leroy, J. Acoust. Soc. Am. **72**, 585 (1982).
[15] T. Kundu, J. Acoust. Soc. Am. **83**, 18 (1988).
[16] N. F. Declercq, J. Degrieck, and O. Leroy, Appl. Phys. Lett. **85**, 148 (2004).
[17] N. F. Declercq, J. Degrieck, and O. Leroy, J. Acoust. Soc. Am. **116**, 51 (2004).
[18] N. F. Declercq, J. Degrieck, and O. Leroy, Acust. Acta Acust. **89**, 1038 (2003).
[19] N. F. Declercq, J. Degrieck, R. Briers, and O. Leroy, Appl. Phys. Lett. **82**, 2533 (2003).
[20] N. F. Declercq, R. Briers, and O. Leroy, Ultrasonics **40**, 345 (2002).
[21] N. F. Declercq, J. Degrieck, and O. Leroy Ultrasonics, **43(4)**, 279–282 (2005).
[22] N. F. Declercq, F. Van den Abeele, J. Degrieck, and O. Leroy IEEE Transactions on Ultrasonics, Ferroelectrics and Frequency Control, 51(10), 1354–1357, (2004).
[23] N. F. Declercq, O. Leroy, J. Degrieck, and J. Vandeputte Acust. Acta

Acust. **90**, 819–829 (2004).
[24]J. Pott and J. G. Harris, J. Acoust. Soc. Am. **76**, 1829 (1984).
[25]A. B. Temsamani, S. Vandenplas, and L. Van Biesen, Ultrasonics **38**, 749 (2000).
[26]T. D. K. Ngoc and W. G. Mayer, J. Acoust. Soc. Am. **67**, 1149 (1980).
[27]M. A. Breazeale, L. Adler, and L. Flax, J. Acoust. Soc. Am. **56**, 866 (1974).
[28]P. B. Nagy, K. Cho, L. Adler, and D. E. Chimenti, J. Acoust. Soc. Am. **81**, 835 (1987).
[29]T. E. Matikas, M. Rousseau, and P. Gatignol, J. Acoust. Soc. Am. **93**, 1407 (1993).
[30]L. E. Pitts, T. J. Plona, and W. G. Mayer, IEEE Trans. Sonics Ultrason. **SU-24**, 101 (1977).
[31]K. W. Ng, T. D. K. Ngoc, J. A. McClure, and W. G. Mayer, Acustica **48**, 168 (1981).
[32]A. N. Norris, J. Acoust. Soc. Am. **73**, 427 (1983).
[33]R. A. Stephen, J. Acoust. Soc. Am. **107**, 1095 (2000).
[34]J. Vandeputte, O. Leroy, R. Briers, and G. Shkerdin, J. Acoust. Soc. Am. **108**, 1614 (2000).
[35]L. W. Couch II, *Digital and Analog Communication Systems*, fifth ed. (Prentice Hall, Englewood Cliffs, NJ, 1997).
[36]H. Nyquist, Trans. AIEE **47**, 617 (1928).
[37]C. E. Shannon, Proc. Institute of Radio Engineers, 37, 10 (1949).
[38]S. Vaezy, B. Huguenin, G. Fleury, J. R. Flexman, and R. Held, Proceedings of 2003 IEEE International Symposium, Honolulu, Hawaii, 5–8 October 2003, paper 2B-3.
[39]M. Tabei, T. D. Mast, and R. C. Waag, J. Acoust. Soc. Am. **113**, 1166 (2003).